Multi-technique characterization of low-temperature plasma nitrided austenitic AISI 304L and AISI 904L stainless steel[†]

Y. Cao,[a]* G. Maistro,[a] M. Norell,[a] S. A. Pérez-Garcia[b] and L. Nyborg[a]

The current study focuses on the characterization of the nitrided layer, formed in American Iron and Steel Institute (AISI) 304L and AISI 904L austenitic stainless steels by industrial low-temperature plasma nitriding, using combined analysis techniques. The study highlighted that the evolution of the microstructure of the nitrided layers is influenced by surface finishing prior to nitriding, alloying elements and nitriding conditions, all factors affecting S-phase formation and nitrogen (N) diffusion mechanisms. The chemical bonding characteristics of Cr $2p_{3/2}$ and N 1s as revealed by XPS show a shift in binding energy between expanded austenite (S-phase) and CrN-like compounds. S-phase has proven to be more stable in 904L, whereas residual and/or induced ferrite/martensite in 304L acts as a barrier for its development. © 2014 The Authors. *Surface and Interface Analysis* published by John Wiley & Sons, Ltd.

Keywords: plasma nitriding; S-phase; stainless; austenitic; XPS

Introduction

Nitriding and carburizing have long been widely used to improve the hardness and tribological properties for many metals and applications. However, conventional thermochemical treatments are not suitable for austenitic stainless steel because the process temperatures are usually high: 850–950 °C for carburizing and 500–550 °C[1] for nitriding. Rapid precipitation of chromium carbides or nitrides depletes chromium in solid solution and impairs substantially the corrosion resistance essential for stainless steels.

In the middle of 1980s, the discovery of the metastable interstitially supersaturated austenite[2], called 'expanded austenite' or 'S-phase', formed in low-temperature processes opened possibilities to challenge this technical issue. Low-temperature nitrided austenitic stainless steel with S-phase can exhibit improved properties, such as increased surface hardness, strength, wear resistance, tribological performance, fatigue resistance, while retaining the anticorrosion properties. The advantageous properties make expanded austenite a promising structure for surface modification of austenitic stainless steel.

One purpose here is to better understand factors affecting the formation of S-phase in plasma nitriding of austenitic stainless steel. Depending on the matrix composition and the nitriding conditions, a 'compound layer' consisting of γ′ phase (Fe_4N), ε compounds ($Fe_{2-3}N$), and Cr nitride can form on the very surface.[1] This might explain the lack of reliable and consistent XPS information for the S-phase in literature. The current study also aims at the clarification of bonding features regarding S-phase and other chemical states.

Experimental

The materials in the current study were American Iron and Steel Institute 304L and 904L (Table 1) austenitic stainless steels ($65 \times 65 \times 3$ mm coupons), respectively having surface finish 2B (cold rolled, heat treated, pickled, and skin passed) and 2E (cold rolled, heat treated, and mechanically descaled) BS EN 10088-2:2005. One sample side was ground and polished using 7 and 3-μm diamond paste prior to nitriding (P), and the other was left nonpolished (N), i.e. as-received. An increased amount of bcc in 304L after polishing was observed with X-ray diffraction (XRD).

Plasma nitriding was performed at 400 °C in H_2/N_2 by Bodycote (Sweden), at different N_2 pressures (labelled H for High and L for Low) and duration (Table 2). Pure H_2 was used at start-up to remove the surface oxides.

Several characterization methods were combined to investigate the nitrided layer, including XPS, XRD, SEM, energy-dispersive X-ray spectroscopy (EDX), and optical microscopy. The phases formed in the nitrided layer were identified by means of Bruker AXS D8 advance XRD system using CrKα radiation ($\lambda = 0.229$ nm) with data acquired for $2\theta = 30$–160°. For XPS analysis, a PHI5500 was used with an AlKα-source and calibrated according to ISO 15472:2001. Depth profiles were obtained by successive XPS analysis and argon ion etchings (4 kV) with rates as calibrated on Ta_2O_5. A LEO Gemini 1550 SEM operated at 20 kV in conjunction with Oxford Inca EDX system was utilized to examine the nitrided layer and Leica optical microscope to examine the top surfaces.

* Correspondence to: Y. Cao, Department of Materials and Manufacturing Technology, Chalmers University of Technology, 41296 Gothenburg, Sweden. E-mail: yu.cao@chalmers.se

[†] Paper published as part of the ECASIA 2013 special issue.

a Department of Materials and Manufacturing Technology, Chalmers University of Technology, 41296 Gothenburg, Sweden

b Centro de Investigación en Materiales Avanzados (CIMAV), Unidad Monterrey, Alianza Nte. 202, Apodaca, Nuevo Leon, 66600, Mexico

Table 1. Chemical composition of AISI 304L and 904L stainless steel

	Fe	C	Mn	Cr	Ni	Mo	Si	S	P	N	Cu	Ti
304L	Bal.	0.019	1.63	18.25	8.05	0.43	0.28	0.001	0.028	0.072	0.33	0
904L	Bal.	0.011	1.62	20.3	24.26	4.37	0.33	0.001	0.023	0.054	1.41	0.007

Table 2. Samples designations, plasma nitriding and layer characteristics

Samples	N_2 partial pressure	Treatment duration (h)	Nitrided layer thickness (μm)	N concentration in S-phase, outer part (at%) (by XPS)
P304L-H	25%	99	39.6 ± 3.9	18–20
N304L-H			44.1 ± 4.1	n.d.
P304L-L	6%	24	4.4 ± 2.0	18–21
N304L-L			8.0 ± 0.5	14–15
P904L-H	25%	99	18.9 ± 2.0	18–20
N904L-H			25.9 ± 3.7	n.d.
P904L-L	6%	24	4.3 ± 0.6	9–10
N904L-L			5.8 ± 1.0	n.d.

H, high N_2 partial pressure; L, low N_2 partial pressure; P, polished surface; N, nonpolished surface; n.d., not determined.

Results

At visual inspection, the polished side of all coupons appear with an opaque circular area in the center of about 30-mm diameter ('area 1') and a mirror-like zone on the rest of the coupon ('area 2') (Fig. 1e), whereas the nonpolished sides had a uniform dull appearance.

Figure 1 a–d shows cross sections from 'L-nitrided' steel. A well-defined nitrided layer was observed in all cases. The thickness and composition of the layer have clearly been affected by factors such as surface roughness, alloying elements and nitriding conditions, as indicated in Table 2. The N concentration was estimated by quantitative XPS analysis after removing the surface compound layer by argon ion sputtering. Compared with high alloyed 904L, 304L has thicker nitrided layer. The thickness also varied somewhat over the coupons, probably due to a nonuniform nitriding process. In the particular case of P304L-L, the S-phase layer thickness ranged from ~8 μm in 'area 1' to ~0 μm in 'area 2', further comparisons will follow. Generally, unpolished surfaces as well as longer nitriding time with increased N_2 content resulted in thicker layers. It was revealed by EDX that in condition H, the N concentration in depth varied only slightly through the layer for both alloys, whereas it decreased to approximately half in condition L.

Top views directly after nitriding, without any chemical etching, are shown in Fig. 2. The austenite grain structure was largely observed on polished samples except for P304L-H (Fig. 2a). Slip bands observed in Fig. 2b and c demonstrate the plastic deformation caused by the stresses due to S-phase formation. Some grains revealed two or more slip systems. Furthermore, the displacement of a preexisting scratch in adjacent areas (see arrow in Fig. 2c) confirmed that twinning occurred during nitriding. Thus, plastic deformation occurred by both gliding and twinning. In addition, high stresses were indicated by micro or macro cracking under H condition, especially for 904L. The austenite grain structure cannot be observed for P304L-H (Fig. 2a). The long process time resulted in partial decomposition of supersaturated S-phase layer as will be described in the succeeding text. It is assumed that the morphology has changed in connection with the decomposition.

As indicated by XRD patterns (Fig. 3a), the nitrided layers on 904L (both H and L conditions) mainly consisted of austenite and S-phase. Generally, the S-phase peaks were broader than the austenite peaks, and asymmetric. The shoulder at the higher angle side of the S-phase indicates the N gradient within the modified layer, characteristic of the L-nitrided samples as observed from EDX experiments. Formation of Cr nitride at the surface was observed by grazing angle incidence (3°) XRD for 904L-L. Polishing prior to plasma nitriding shifted the S-phase peaks in 904L-L towards higher 2θ angles, corresponding to less expanded structure. Compared with P904L-L, the S-phase peaks in P904L-H shifted towards lower 2θ angle due to the increased layer thickness and higher average N concentration.
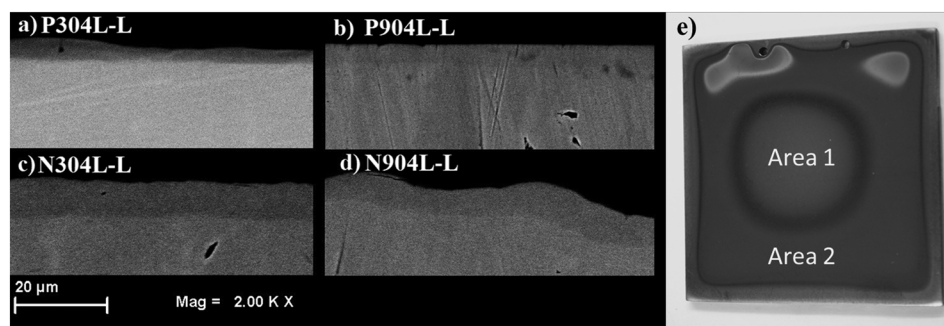

Figure 1. (a–d) Backscattered electrons image of the cross section from nitrided steels and e) top view photo of the polished and nitride P904L-L.
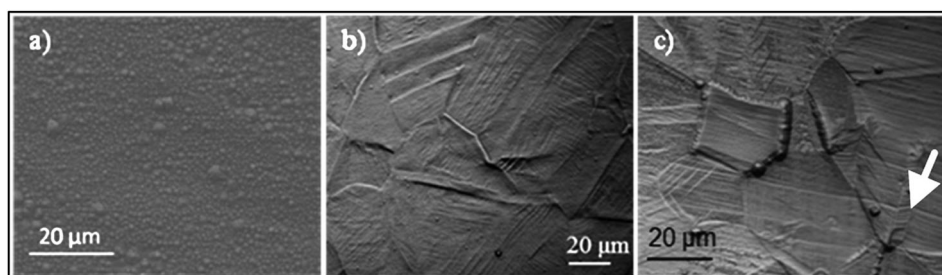
Figure 2. a) SEM top view from as-nitrided P304L-H; b and c) Optical top view from as-nitrided; b) P904L-L; c) as-nitrided P904L-H.
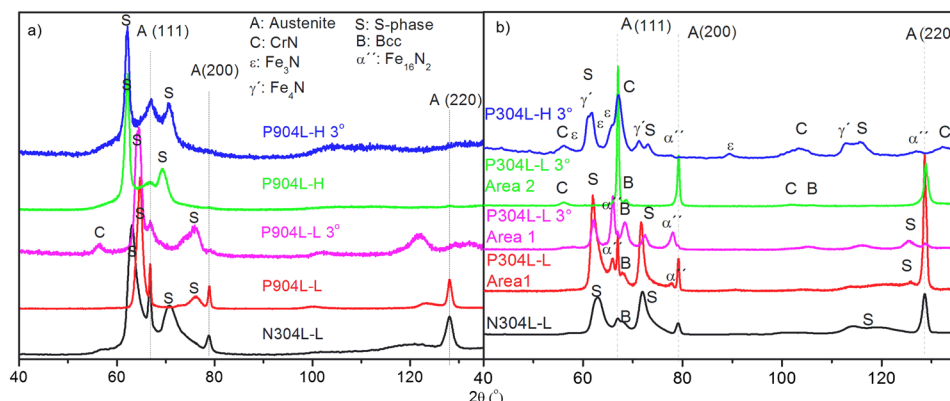

Figure 3. XRD pattern from as-nitrided materials a) 904L and b) 304L.

The XRD pattern of P304L-H was more complicated (Fig. 3b). Formation of bcc iron, CrN-like nitride, γ' (Fe$_4$N) and/or ε (Fe$_3$N) compounds indicated that the S-phase was less stable than in 904L. S-phase decomposition into bcc iron and nitride reduces internal stresses consistent with Fig. 2a where no twins or slip bands are observed. The XRD pattern for polished P304L-L ('area 1' in Fig. 3b) suggested the formation of nitride α'' (Fe$_{16}$N$_2$) instead of γ' or ε compound. Jack ascribed it to a transition phase prior to Fe$_4$N in a study regarding decomposition of N containing martensite.[3] Grazing angle incidence XRD indicated a large amount of α'' together with CrN developed at the surface. As previously mentioned, the nitrided layer on P304L-L was thicker in 'area 1' than in 'area 2'. In 'area 2', CrN-like compounds were clearly identified in grazing angle configuration. However, no nitride was recorded from nonpolished N304L-L. A strong single broad peak representing S-phase appeared left of the low angle austenite peak, whereas it splitted to double peaks at higher 2θ angle. This confirmed again the positive effect of the rough surface on the formation of S-phase.

Figure 4 shows XPS depth profiles of the nitrided layers on polished surface. It was found that a compound layer was present in all conditions, but the thickness varied between samples. Sometimes, it was too thin to be identified with XRD. Because the O content in the S-phase was very low, and to clarify the distribution of the other elements, O is not shown in Fig. 4. However, from the XPS analyses, it appeared that a small amount (~5 atomic %) of O may incorporate into the surface compound, and occasionally, an O enrichment up to 20 at-% was noted at the interface between the compound layer and the S-phase. In all cases, the N profile followed Cr, and the N/Cr atomic ratio was close to 1. Two representative profiles from P304L-L are presented in Fig. 4a and b. A clear Cr and N rich layer (~140 nm) was observed from 'area 2'. This was consistent with the formation

of Cr nitride as revealed by XRD pattern. In 'area 1' with thicker S-phase, only a thin (~10 nm) enrichment of Cr and N was detected. However, as indicated by the XRD pattern, α'' was present below this layer. Cr nitride layer (~70 nm) was also recorded for P904L-L (Fig. 4d). Table 3 summarizes the compound layer thickness estimated from the depth where half the N intensity decrease occurred. Together with XRD results, it can be concluded that high alloying content and increased N$_2$ content in the nitriding gas mixture led to thinner compound layer, despite longer nitriding time.

Controlled polishing was performed to completely remove thin compound layers while maintaining thick ones. This allowed for XPS studies of compound and S-phase with only limited ion etching to remove surface contamination while minimizing beam damage. In P904L-H, the compound layer was so thin that 30-s polishing using 1-μm diamond paste was sufficient to remove it (as shown by hollow points in Fig. 4c). Figure 5 shows XPS results from as-nitrided materials after 1-min mechanical polishing followed by 120 s of low energy ion etching (1 keV, to remove surface contamination while minimizing beam damage). After this procedure, the surface on P904L-H is supposed to be S-phase, according to XRD and XPS depth profiling, and its Cr 2p$_{3/2}$ and N 1s peaks were located at 574.5 and 397.3 eV, respectively. For all other samples, corresponding to CrN-like compound, the Cr 2p$_{3/2}$ peaks were at the same binding energy (BE). With respect to Cr 2p$_{3/2}$ line for metal state, the core level shift ΔEc was 0.5 eV for S-phase and 0.8 eV for CrN-like compound. On the other hand, in comparison with that of S-phase, the N 1s peak for CrN in P904L-L moved to lower BE by 0.3 eV (Fig. 5b). It seemed that the chemical shift of N 1s between α'' nitride (P304L-L) and CrN was insignificant.

Moreover, the asymmetric high BE tail of N 1s observed in P304L-H can probably be attributed to Fe-N bonding from γ'
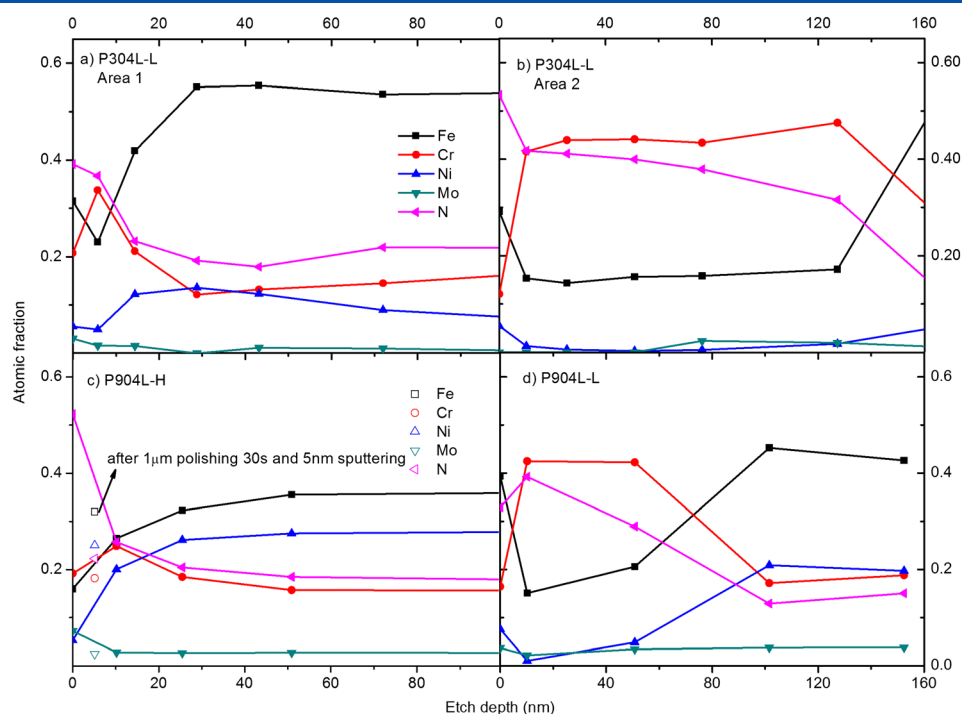
Figure 4. XPS profiles of the nitrided layers on polished surface.

Table 3. Estimated surface compound layer thickness (nm)

Sample	P904L-H	P304L-L	P904L-L
Thickness	~6	>10$^{Area\ 1}$/140$^{Area\ 2}$	~70

and ε. This result is in good agreement with the XRD patterns collected both in grazing angle and in θ/2θ configurations. Also, XPS indicated that Ni was always present in metallic state.

Discussion

The surface state prior to nitriding, alloying elements present in the material and nitriding parameters significantly affect the thickness and microstructure of the case layer.

As shown in Fig. 2, the stresses caused by the S-phase formation induced plastic deformation not only by gliding at lower strains, but also twinning at higher strains. Twinning has long been observed in the mechanical deformation of nitrogen-alloyed steel.[4] Generally, nitrogen decreases the stacking fault energy (SFE),[5,6] promoting the formation of stacking faults (SF)[7] and consequently mechanical twinning. Although effects of alloying elements on SFE might not be monotonous and interaction exists among different elements in austenitic stainless steel,[8] truly the SFE in austenitic stainless steel is relatively low.[6] SFs, enhanced by high nitrogen content, are an inherent feature of the S-phase contributing also to the broadening and shifting of XRD peaks in S-phase.[2]

The nucleation and subsequent growth of surface nitride are determined by the competition between the N flux arriving at the surface and the flux of those leaving the surface. When the former one is prevailing and the surface N concentration exceeds the solubility limit, a surface compound layer will be developed after an incubation time. The process parameters are crucial to the formation of this layer. It has been reported[9,10] that the N occupancy (concentration) in the fcc lattice increases with the N activity a_N in the gas mixture. Meanwhile, the diffusion coefficient
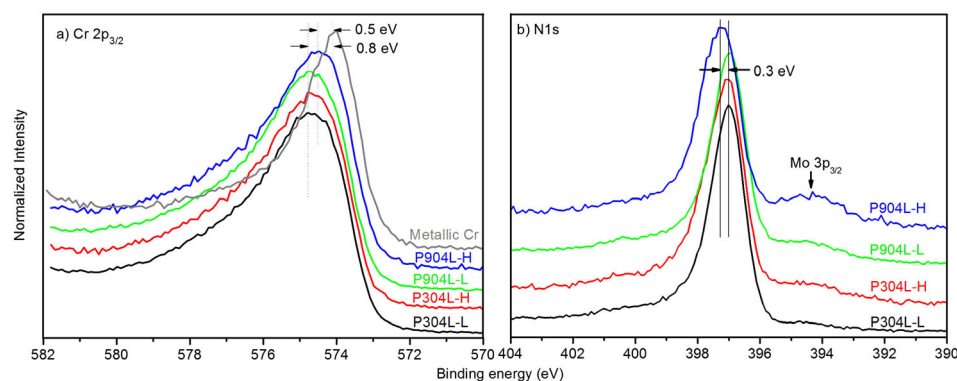

Figure 5. XPS a) Cr 2p$_{3/2}$ and b) N 1s peaks from as-nitrided materials.

of N in S-phase is concentration-dependent and high N content gives high diffusivity until a N occupancy of 0.45.[9] Calculations by Mändl *et al.*[11] indicate a steep increase of the diffusivity at 17 at% N for 304 steel. In the current study, the reduced N_2 partial pressure in the L condition resulted in lower a_N (nitriding potential) and consequently smaller average N content in the nitrided materials, giving rise to lower N diffusivity, and this is believed to promote the formation of surface compound in comparison with the H condition.

The surface state prior to plasma nitriding affects the nitrided layer. The starting materials had surface finish 2B (cold rolled, heat treated, pickled, and skin passed) for 304L and 2E (cold rolled, heat treated, and mechanically descaled) for 904L, respectively. The presence of surface defects coming from the surface finish treatment enhances the nitrogen diffusion rate. Removing this layer, at least partly by polishing, led to a thinner nitrided layer. After plasma nitriding, compressive surface residual stresses are built up at and below the surface. The higher penetration depths of N in as-received nonpolished samples are also associated with the easier relaxation of nitriding-induced compressive residual stresses at the surface owing to the increased free surface area caused by the increased roughness.

Alloy composition plays significant roles on the S-phase formation. As a strong nitride former, Cr has the highest affinity for N, enables N permeation into austenite and is essential for the development of S-phase.[2] Compared with 304L, 904L contains three times more Ni and ten times more Mo. The increased S-phase stability in 904L is attributed to Ni, being an effective austenite stabilizer.[12] Meanwhile, large Mo atoms widen the octahedral sites and enable quicker diffusion of N. However, extremely low affinity between Ni and N slows down the growth of S-phase, leading to thinner layers on 904L.

It is generally accepted that S-phase formation is less likely for ferritic stainless steels.[2] The significant thickness variation between 'area 1' and 'area 2' in P304L-L could partly be explained as follows. For as-received original 304L, a small amount of bcc α phase was identified in the XRD pattern. Domains with higher Cr content (~26 at%) has been confirmed by SEM and EDX (not shown here). After polishing, an increased amount of bcc in 304L was observed with XRD, corresponding to deformation induced martensite. Such ferrite/martensite was not observed in 904L. The presence of the ferrite (in the original alloy) and martensite (induced by mechanical polishing) makes the alloy more sensitive to the inhomogeneity of the plasma nitriding process. Consequently, at the location where the plasma is 'weaker' (area 2) in this industrial process, the formation of S-phases is limited.

There are two possible modes of nitride formation in 304L. In the first, precipitation of CrN-like compound which has higher stability than Fe nitride occurs. Subsequently, because of a high flux of N and limited diffusion rate for Cr, local enrichment of N will also facilitate the development of γ' and/or ε compound. The second mode involves decomposition of metastable S-phase into stable nitrides when exposed to temperatures above a certain value. In austenitic stainless steels, for temperatures above 450 °C, the presence of CrN and α-Fe along with γ' and ε compounds has been reported.[2,13] In our study, the nitrides present inside the layer are believed to arise from partial decomposition of supersaturated S-layer, producing a mixture of bcc iron and nitride in H condition. This decomposition continued when the nitrided samples were subsequently heated at 450 °C.[14] Transition nitrides (α'') may have occurred as an intermediate in the decomposition.

It is normally accepted that preferential bonding of Cr with N is formed in S-phase. With respect to its metal state, the Cr $2p_{3/2}$ peak in S-phase shifts 0.5 eV to higher BE. This is consistent with

the reported value for Cr–N bonding.[15] The recorded shift of CrN-like compound (0.8 eV) is in the range of literature values for CrN (0.5–1.5 eV).[16,17] It should be mentioned that diffraction lines assigned as CrN in the XRD pattern (Fig. 3) are broad and exhibits some shift from the standard XRD powder patterns, implying a deviation from the ideal CrN structure. On the other hand, XPS depth profiles (Fig. 4) always demonstrate considerable Fe content through the layer that would affect the structure. Interestingly, it has been reported that S-phase layer thickness increases in the sequence of Ni–Cr, Co–Cr, and Fe–Cr-based alloys,[2] indicating that the role of Fe in the S-phase formation cannot be ignored. Fe–N bonding feature in both S-phase and nitrides is a matter of great interest for future detailed and systematic XPS studies of CrN-like compounds.

Conclusions

Expanded austenite supersaturated with N, or S-phase, formed on industrial low-temperature plasma nitrided surfaces of alloys 304L and 904L. SEM cross sections, EDX, XRD, and XPS analysis show that polishing, shorter nitriding time, and reduced N_2 content in the gas lead to thinner S-phase layers. The S-phase on 904L is more stable but thinner than that on 304L. A thick or thin compound layer at the very surface is often observed at least by XPS, and this is related to the initial stage of the plasma nitriding mechanisms.

The high stresses owing to the S-phase formation lead to plastic deformation by both gliding in two or more slip systems and twinning. With respect to the Cr $2p_{3/2}$ line for metal state, the core level shift ΔEc is 0.5 eV for S-phase and 0.8 eV for CrN-like compound. In comparison with that of S-phase, N 1s peak for CrN-like compound is moved to lower BE by 0.3 eV.

References

[1] D. Pye, Steel Heat Treatment Metallurgy and Technologies, CRC Press, Boca Raton (FL), **2006**.
[2] H. Dong, *Int. Mater. Rev.* **2010**, *55*(2), 65.
[3] K. H. Jack, *Proc. R. Soc. London, Ser. A* **1951**; *208*(1063), 200. DOI: 10.1098/rspa.1951.0154
[4] P. Müllner, C. Solenthaler, P. Uggowitzer, M. O. Speidel, *Mater. Sci. Eng. A* **1993**, *164*, 164.
[5] X. Xu, L. Wang, Z. Yu, J. Qiang, Z. Hei, *Metall. Mater. Trans. A* **2000**, *31A*, 1193.
[6] J. Liu, P. Han, M. Dong, G. Fan, G. Qiao, J. Yang, *Physica B.* **2012**, *407*, 891–895.
[7] J. C. Jiang, E. I. Meletis, *J. Appl. Phys.* **2000**, *88*, 4026.
[8] L. Vitos, J.-O. Nilsson, B. Johansson, *Acta Mater.* **2006**, *54*(14), 3821.
[9] M. A. J. Somers, T. Christiansen, *J. Phase Equilib. Diffus.* **2005**, *26*(5), 520.
[10] T. Christiansen, M. A. J. Somers, *Metall. Mater. Trans. A.* **2006**, *37A*, 675.
[11] S. Mändl, B. Rauschenbach, *J. Appl. Phys.* **2002**, *91*, 9737.
[12] C. Blawert, B. L. Mordike, Y. Jiraskova, O. Schneeweiss, *Surf. Coat. Technol.* **1999**, *116-119*, 189.
[13] M. P. Fewell, D. R. G. Mitchell, J. M. Priest, K. T. Short, G. A. Collins, *Surf. Coat. Technol.* **2000**, *131*, 300.
[14] Y. Cao, M. Norell, *Oxid. Met.* **2013**, *80*(5-6), 479
[15] E. Menthe, K.-T. Rie, J. W. Schultze, S. Simson, *Surf. Coat. Technol.* **1995**, *74-75*, 412.
[16] C. D. Wagner, W. M. Riggs, L. E. Davis, J. F. Moulder, Handbook of X-Ray Photoelectron Spectroscopy, Perkin Elmer Corporation, Eden Prairie (MN), **1979**.
[17] G. S. Chang, J. H. Son, S. H. Kim, K. H. Chae, C. N. Whang, E. Menthe, K.-T. Rie, Y. P. Lee, *Surf. Coat. Technol.* **1999**, *112*, 291.